FINITE ELEMENT MODELING AND ANALYSIS OF RADIO FREQUENCY HEATING RATE IN MUNG BEANS

Z. Huang, H. Zhu, S. Wang

ABSTRACT. *Radio frequency (RF) heating has been extensively studied as a novel disinfestation method for dry agricultural products. A major difficulty in using this method is that different heating rates at the corners and edges of materials may cause negative effects on product quality. A systematic analysis of factors that influence the RF heating rate is desirable to help in designing effective treatment protocols. A finite element model using COMSOL Multiphysics software was developed and experimentally validated with 3 kg of mung beans in a 6 kW, 27.12 MHz free-running oscillator RF system to study the influence of sample moisture content, density, specific heat capacity, thermal conductivity, dielectric properties, top electrode voltage, and electrode gap on RF heating rate. Simulation results demonstrated that the variation in sample density and specific heat capacity, especially thermal conductivity, had a relatively slight effect on RF heating rate. The RF heating rate was significantly influenced by electrode gap, top electrode voltage, and the dielectric properties and moisture content of the sample. These heating rate distributions might be valuable in guiding and optimizing RF treatment conditions, which are helpful to improve RF heating uniformity for disinfecting dry products.*

Keywords. *Dielectric properties, Finite element modeling, Heating rate, Mung bean, Radio frequency.*

China is a major producer and exporter of mung beans in the world, with an annual production of 952,000 metric tons in 2011, about 12% of which was for the export market (Hui and Ninghui, 2013). Mung beans are widely used in the food (carbohydrate, fat, protein, and starch), pharmaceutical (amino acids, antinutritional factors, minerals, and vitamins), and brewing (moisture and saccharine) industries due to their high economic value. The chemical composition of mung beans is reported as 4.3 g $(100\ g)^{-1}$ ash, 59.8 g $(100\ g)^{-1}$ carbohydrate, 1.1 g $(100\ g)^{-1}$ crude fat, 4.3 g $(100\ g)^{-1}$ fiber, 26.4 g $(100\ g)^{-1}$ protein, 142 mg $(100\ g)^{-1}$ calcium, 6.8 mg $(100\ g)^{-1}$ iron, 1032 mg $(100\ g)^{-1}$ potassium, 287 mg $(100\ g)^{-1}$ phosphorus and 11.8 mg $(100\ g)^{-1}$ sodium (Amarteifio and Moholo, 1998). However, infestation by insect pests is a major problem in the harvesting, processing, and marketing of mung beans. Insects reduce the quality of mung beans through direct damage, contamination with fecal matter, and webbing (Pimentel, 2002). Infested mung beans are not easily detected by visual inspection, leading to a serious threat for quarantine regulations and consumer health. Traditionally, fumigation with methyl bromide (MeBr) has been the most widely used treatment for postharvest insect control in the legume industry due to its high efficacy and relatively low cost (Barreveld, 1993; Carpenter et al., 2000). The major drawback of MeBr fumigation is the negative environmental impact due to depletion of the ozone layer, resulting in increased demand for nonchemical pest control methods in the legume industry (Osteen, 2000). A potential alternative to chemical methods is radio frequency (RF) treatment, which has been shown to be an environmentally friendly technology for insect control in mung beans without degrading product quality (Nelson, 1996; Wang et al., 2007b, 2010; Jiao et al., 2012).

RF dielectric heating is an electromagnetic wave treatment that can rapidly raise the internal sample temperature volumetrically. Polar molecule rotation and charged ion movement are the two main contributors to RF heat generation, which can increase the heating rate, reduce treatment time, and maintain better quality in bulk materials as compared to conventional thermal treatment methods (Piyasena et al., 2003). Many studies have explored the possibility of using RF energy to disinfest produce with insect pests (Hallman and Sharp, 1994; Mitcham et al., 2004; Lagunas-Solar et al., 2007; Shrestha and Baik, 2013). RF energy has been used for disinfesting legumes, such as chickpeas (Johnson et al., 2010), green peas (Wang et al., 2010), black-eyed peas, and lentils (Wang et al., 2008b; Jiao et al., 2012). Treatment conditions of 55°C to 58°C for 5 to 10 min have been successfully applied to achieve 100% insect (cowpea weevil) mortality without major effects on legume (chickpea, green pea, and lentil samples) color, weight loss, and germination (Johnson et al., 2004; Wang et al., 2010; Jiao et al., 2012). However, the major challenge with RF heating of dry agricultural products is overheating

Submitted for review in March 2014 as manuscript number PRS 10660; for publication by the Processing Systems Community of ASABE in December 2014.

The authors are **Zhi Huang, ASABE Member,** Graduate Student, and **Hankun Zhu, ASABE Member,** Graduate Student, College of Mechanical and Electronic Engineering, Northwest A&F University, Yangling, China; **Shaojin Wang, ASABE Member,** Professor, College of Mechanical and Electronic Engineering, Northwest A&F University, Yangling, China, and Adjunct Professor, Department of Biological Systems Engineering, Washington State University, Pullman, Washington. **Corresponding author:** Shaojin Wang, College of Mechanical and Electronic Engineering, Northwest A&F University, 22 Xinong Road, Yangling, Shaanxi 712100, China; phone: +86-29-87092319; email: shaojinwang@nwsuaf.edu.cn.

of corners and edges, resulting in non-uniform and runaway heating (Ikediala et al., 2002; Piyasena et al., 2003).

Differential heating rates in RF-treated samples are a major concern for ensuring complete control of insects and providing acceptable product quality, which can be reduced by uneven distribution of the electromagnetic field (Wang et al., 2008a). High product temperatures may result in poor quality, such as oil rancidity in nuts (Wang et al., 2007a) and visible heat damage in fruits (Birla et al., 2004). Thus, understanding the influence of various factors on heating rates in mung beans is essential to provide practical RF treatment parameters and minimize adverse effects on product quality.

Since experimental methods are time consuming and costly, computer simulation methods play an important role in understanding RF heating behavior and have been effectively used since the 1990s (Neophytou and Metaxas, 1996, 1998). Several authors have used commercial simulation methods to solve combined wave (or Laplace) and heat transfer equations to develop the electromagnetic and temperature fields (Yang et al., 2003; Chan et al., 2004; Marra et al., 2007). Romano and Marra (2008) simulated RF heating of a cylindrical luncheon meat roll in a 600 W RF oven operated at 27.12 MHz. Birla et al. (2008) successfully simulated the non-uniform RF heating of fresh fruits using FEMLAB. Tiwari et al. (2011a) simulated RF heating of wheat flour packed inside rectangular polypropylene containers in a 12 kW, 27.12 MHz RF system with a Joule heating model using COMSOL Multiphysics software and applied the validated model to predict the influence of various factors on the RF power density distribution in dry food materials (Tiwari et al., 2011b). Alfaifi et al. (2014) developed a computer simulation model by using a Joule heating model in COMSOL and validated the computer model with experimental temperature profiles of raisins in a 6 kW, 27.12 MHz RF system. Zhu et al. (2014) simulated the top electrode voltage using COMSOL with 3 kg of soybeans in a 6 kW, 27.12 MHz RF system and established a correlation between the electrode voltages and currents. Huang et al. (2015) developed a computer simulation model for dry soybeans using COMSOL and applied the validated simulation model to predict the effects of different treatment conditions on RF heating uniformity. To our knowledge, no parametric studies have been conducted on the influence of product properties and RF processing conditions on mung bean heating rate.

The objectives of this study were to develop a computer simulation model using COMSOL Multiphysics software, validate the computer simulation model with 3 kg of mung beans in a 6 kW, 27.12 MHz free-running oscillator RF system, and analyze the influence of various factors (e.g., moisture content, density, specific heat capacity, dielectric properties, and thermal conductivity of the samples, as well as electrode gap and top electrode voltage) on RF heating rate using the validated simulation model.

MATERIALS AND METHODS

SAMPLE PREPARATION

Mung beans were purchased from a local grocery store in Yangling, Shaanxi, China. The initial moisture content of the mung beans was 7.54% ±0.03% on wet basis (w.b.). The samples were maintained at 20°C ±0.5°C in a thermostatic and humidity (52% RH) controlled chamber (BSC-150, Shanghai BoXun Industrial & Commerce Co., Ltd., Shanghai, China) for 24 h prior to the RF experiments. The bulk density of the mung beans at room temperature was measured with a basic volume method using a 300 mm × 220 mm × 50 mm container (Jiao et al., 2011b) and determined to be 953 ±6 kg m^{-3} based on three replicates.

COMPUTER SIMULATION

Physical and Geometry Model

A 6 kW, 27.12 MHz pilot-scale RF heating system (SO6B, Strayfield International, Ltd., Wokingham, U.K.) was used to determine the heating rate and temperature distribution in mung beans. The RF system included a metallic enclosure, a generator, and a pair of RF electrodes. The top electrode could be adjusted to achieve the required RF power (Tiwari et al., 2011a). Figure 1 shows a schematic diagram of the RF heating system. In this study, mung beans in a plastic container (300 mm × 220 mm × 50 mm) were placed on the center of the bottom electrode. The gap between the two electrodes was fixed at 120 mm to achieve an appropriate heating rate based on a previous study (Jiao et al., 2012).

Governing Equations

The governing equations include electromagnetic and heat transfer partial differential equations, which need to be solved simultaneously. The applied electric field at any point inside a food material is governed by a quasi-static approximation of Maxwell's equations as (Choi and Konrad, 1991):

$$-\nabla \cdot \left[\left(\sigma + j 2\pi f \varepsilon_0 \varepsilon' \right) \nabla V \right] = 0 \tag{1}$$

where $j = (-1)^{0.5}$, f is the frequency (Hz), σ is the electric conductivity (S m^{-1}), ε_0 is the relative permittivity of a vacuum (8.854×10^{-12} F m^{-1}), ε' is the relative dielectric constant of the food material, V is the electric potential (V), and $\vec{E} = -\nabla V$ is the applied electric field strength (V m^{-1}).

The absorbed RF power raises the temperature of the food sample, so heat transfer takes place inside the food and between the food and its surroundings, and is governed by the transient heat transfer equation as:

$$\rho C_P \frac{\partial T}{\partial t} = \nabla (k \nabla T) + P \tag{2}$$

where ρ is the density of the material (kg m^{-3}), C_p is the specific heat capacity of the material (J kg^{-1} °C^{-1}), $\partial T/\partial t$ is the heating rate (°C s^{-1}), k is the thermal conductivity (W m^{-1} °C^{-1}), and P is the power conversion in the food material from electro-

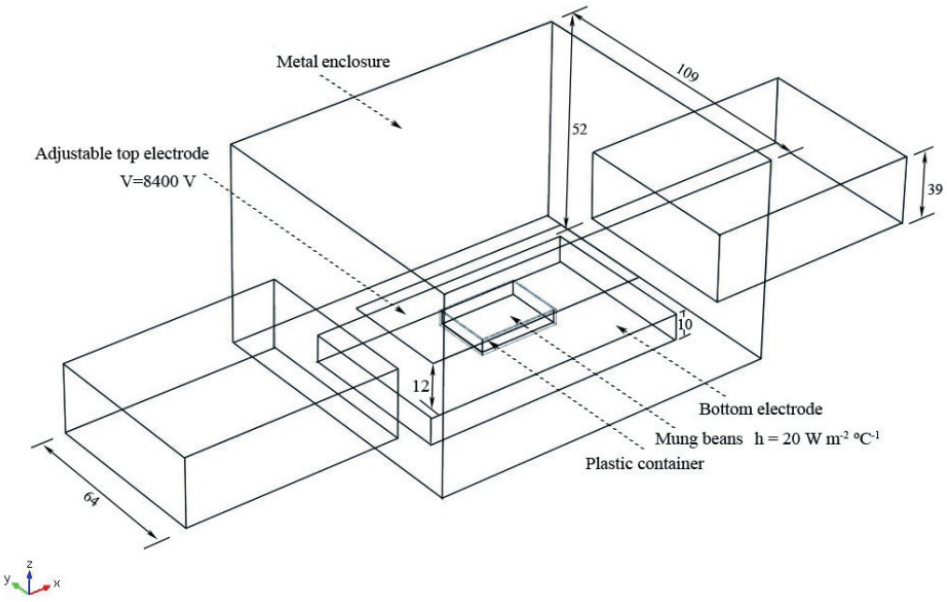

Figure 1. Schematic diagram of the 6 kW, 27.12 MHz radio frequency heating system (all dimensions are in cm).

magnetic to thermal energy (W m^{-3}). Heat loss due to airflowis modeled by specifying the convective heat transfer coefficient at the surface of the sample, and the boundary conditions are defined as:

$$-k\nabla T = h\left(T - T_a\right) \tag{3}$$

where h is the surface heat transfer coefficient (W m^{-2} °C^{-1}), and T_a is the ambient temperature (°C). For a given electric field intensity, P is defined as (Barber, 1983; Metaxas, 1996):

$$P = 2\pi f \varepsilon_0 \varepsilon'' \left|\vec{E}\right|^2 = \sigma \left|-\nabla V\right|^2 \tag{4}$$

where ε'' is the loss factor of the food material, $\sigma = 2\pi f \varepsilon_0 \varepsilon''$ is the effective electric conductivity of the food load (S m^{-1}), and $-\nabla V$ is obtained from equation 1, which performs as the coupling equation of equations 2 and 4 for computing the time-dependent temperature distribution. The electrical ($-\sigma \nabla V = 0$) and thermal insulating ($-k\nabla V = 0$) boundary conditions were applied to the outer surfaces of the RF applicator (fig. 1). The bottom electrode and RF cavity walls were grounded ($V = 0$ V). The convective heat transfer of the sample on the top exposed surface was set as h = 20 W m^{-2} °C^{-1} (fig. 1). Initial temperature was set at room temperature (20°C).

The heating rate inside the food material can be calculated from equation 2 assuming $\rho C_p \neq 0$:

$$\frac{\partial T}{\partial t} = \alpha \nabla^2 T + \frac{P}{\rho C_p} \tag{5}$$

where $\alpha = k/(\rho C_p)$ is the thermal diffusivity of the heated material (m^2 s^{-1}), which is a parameter associated with transient heat flow that governs the temperature variation within a product.

When the heat loss to ambient air is negligible, equation 5 can be written as (Jiao et al., 2014a):

$$\frac{\partial T}{\partial t} = 2\pi f \varepsilon_0 V^2 \frac{\varepsilon''}{\rho C_p \left[\left(\varepsilon' d_0 + d_m\right)^2 + \left(\varepsilon'' d_0\right)^2\right]} \tag{6}$$

where d_0 is the air gap between the top electrode and the upper surface of food material (m), and d_m is the height of the sample (m). According to equation 6, the final temperature after RF heating can be described as:

$$\begin{aligned} T_f &= T_i + t \cdot \frac{\partial T}{\partial t} \\ &= T_i + t \cdot 2\pi f \varepsilon_0 V^2 \frac{\varepsilon''}{\rho C_p \left[\left(\varepsilon' d_0 + d_m\right)^2 + \left(\varepsilon'' d_0\right)^2\right]} \end{aligned} \tag{7}$$

where T_f and T_i are the final and initial temperatures of the sample (°C), and t is the total heating time (s).

The average temperature (T_{avg}, °C) in a dielectric material is defined as the volume integral of the final temperature (T_f, °C) divided by the material volume (V_{vol}, m^3) as follows (Tiwari et al., 2011b):

$$\begin{aligned} T_{avg} &= \frac{1}{V_{vol}} \int_{V_{vol}} T_f \, dV_{vol} \\ &= \frac{1}{V_{vol}} \int_{V_{vol}} \left(T_i + t \cdot \frac{\partial T}{\partial t}\right) dV_{vol} \end{aligned} \tag{8}$$

The temperature uniformity index (TUI) is a useful tool to evaluate the heating uniformity of treated samples in simulations when using a specific RF unit (Alfaifi et al., 2014; Huang et al., 2015):

$$\mathrm{TUI} = \frac{\frac{1}{V_{vol}} \int_{V_{vol}} \mathrm{sqrt}\left[\left(T_f - T_{avg}\right)^2\right] dV_{vol}}{T_{avg} - T_i} \tag{9}$$

It is clear that the RF heating uniformity is directly influenced by the final and average temperatures from equa-

Table 1. Dielectric and thermal properties of materials used in computer simulation.

Material Property	Mung Beans	Aluminum[a]	Air[a]	Polypropylene[a]
Density (kg m^{-3})	953	2700	1.2	900
Thermal conductivity (W m^{-1} °C^{-1})	0.102[b]	160	0.025	0.26
Heat capacity (J kg^{-1} °C^{-1})	$18T + 1165$[b]	900	1200	1800
Dielectric constant	$0.021T + 1.82$[c]	1	1	2.0
Loss factor	$0.0028T + 0.036$[c]	0	0	0.0023

[a] Source: COMSOL material library (COMSOL, 2012).
[b] Source: Ravikanth et al. (2012); T = temperature (°C).
[c] Source: Jiao et al. (2011a); T = temperature (°C).

tion 9, which are affected by the heating rates from equations 7 and 8. If the individual heating rates could be determined at different locations in the sample of the container, these relationships could be used to analyze the RF heating uniformity as influenced by the heating rate changes caused by the studied parameters.

As the dimension of the top electrode (0.83 m × 0.40 m^2) was less than 30% of the RF wavelength (11 m) at 27.12 MHz, its voltage was assumed to be uniformly distributed (Marra et al., 2007; Tiwari et al., 2011a, 2011b). Because the voltage at different load positions in industrial RF systems varies less than 7%, the top electrode voltage could be considered as a constant. When heat loss from mung beans to ambient air is negligible, the top electrode voltage can be estimated by the following equation (Birla et al., 2008):

$$V = \left(d_0 \sqrt{(\varepsilon')^2 + (\varepsilon'')^2} + d_m \right) \left(\sqrt{\frac{\rho c_p}{\pi f \varepsilon_0 \varepsilon''} \frac{dT}{dt}} \right) \quad (10)$$

The estimated voltage for the simulation was 8400 V, based on the heating rate in preliminary tests. The gap between the electrodes was set as 120 mm to heat the sample center from 20°C to 50°C or 53°C, at a heating rate of 5 to 6 °C min^{-1}. These operating conditions have been found to be appropriate for disinfestation of cowpea weevil (*Callosobruchus maculatus*), one of the most resistant insects in mung beans (Jiao et al., 2011b). Sample density and thermal conductivity were assumed to be temperature-independent due to negligible changes over the small temperature range from 20°C to 60°C. This temperature has been documented to be suitable for postharvest pest control (Jiao et al., 2011a). The specific heat capacity and dielectric properties of the material were presumed to be temperature-dependent and were obtained from Ravikanth et al. (2012). Table 1 summarizes the properties of the various materials used in the computer simulations.

Solving Procedure

The models were implemented in COMSOL Multiphysics software (COMSOL, 2012) based on a finite element method. A Dell workstation with two Dual Core i5-2400, 3.10 GHz Xeon processors and 8 GB RAM running a Windows 7 64-bit operating system was used to run the software. A Joule heating model, which coupled the heat transfer and electric current models, was developed. The physics-controlled mesh option (extremely fine mesh) was used for meshing the solution domain. The final mesh system consisting of 43,706 domain elements (tetrahedral), 7,480 boundary elements (triangular), 672 edge elements (linear), and 53 endpoint elements was adopted in subsequent calculations. The time-dependent solver of UMFPACK with an absolute tolerance of 0.01 was used to solve the equations. The maximum time steps were set as 1 s. Total solution time depended on the simulation sequence and varied from 15 to 30 min.

MODEL VALIDATION: RF HEATING EXPERIMENTS

To validate the simulation results, a rectangular container (300 mm L × 220 mm W × 50 H mm) filled with 3 kg of mung beans was placed on the center of the bottom electrode of the RF system. The mung bean sample was divided into three layers at heights of 1.7, 3.4, and 5.0 cm using thin plastic film so as to obtain the sample surface temperature distributions in each layer (Huang et al., 2015). The gap between the two electrodes was fixed at 120 mm. During RF heating, the center temperature of the second layer was measured with a fiber optical sensor (HQ-FTS-D120, Xi'an HeQi Opto-Electronic Technology Co., Ltd., Shanxi, China) with an accuracy of ±1°C (fig. 2) and recorded with a data logger (FTS-P104, Xi'an HeQi Opto-Electronic Technology Co., Ltd.). These heating rate data were then used to estimate the voltage of the top electrode using equation 10. After RF heating for the predetermined time of 6 min, the RF unit was turned off and the container was removed immediately for surface temperature mapping with an infrared camera (DM63-S, DaLi Science and Technology Co., Ltd., Zhejiang, China) with an accuracy of ±2°C. Thermal images were taken from the top layer, followed by the middle and bottom layers. The total measurement time for the three layers was about 30 s. The temperatures in the three different layers were analyzed using an image analysis system (V1.0, DaLi Science and Technology Co., Ltd.). Contour plots were used to present isothermal curves of the temperature distributions in the three layers to compare with the simulation results. Figure 2 shows the experimental setup for sample temperature

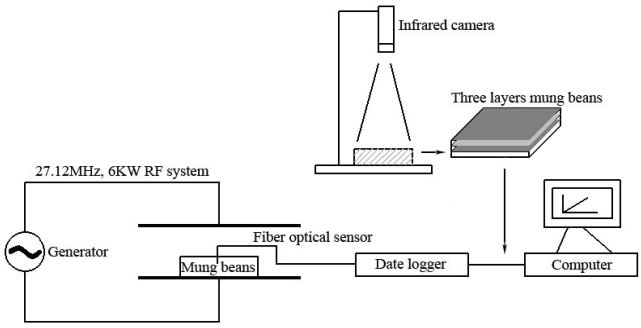

Figure 2. Experimental setup for sample temperature measurements in radio frequency heating.

measurements during RF heating. Heating experiments were replicated five times.

Simulation Applications

Effects of Sample Physical Properties on RF Heating Rate

Thermal conductivity, specific heat capacity, and density are the primary thermal properties of products that influence RF heating rates and are therefore important when simulating heat transfer phenomena during RF heating. To study the effects of these parameters on RF heating rate (using 6 min RF heating and electrode gap of 120 mm), simulations were performed by varying (1) sample moisture content from 6% to 22% w.b., (2) sample density from 800 to 1200 kg m^{-3}, and (3) the specific heat capacity from 1400 to 2200 J kg^{-1} $°C^{-1}$ at five moisture content levels (6%, 10%, 14%, 18%, and 22% w.b.) (Jiao et al., 2011b). Values of the thermal conductivity of mung beans varying from 0.08 to 0.16 W m^{-1} $°C^{-1}$ were used in the simulation model, which could be considered the possible range based on the real thermal conductivity values (0.102 W m^{-1} $°C^{-1}$).

Effects of Sample Dielectric Properties on RF Heating Rate

The dielectric properties of a given material are usually a function of frequency, temperature, density, moisture content, and other properties of the material (Berbert et al., 2002). Values of the dielectric properties may change during the RF heating process, and the heating behavior may vary accordingly. Therefore, knowing the relationship between heating rate and dielectric properties before conducting experiments may help to predict the temperature changes in bulk products and to better understand the RF heating process. To obtain a uniform temperature distribution in foods, a uniform electric field needs to be generated throughout the treated food sample. It is well known that if the loss factor is far smaller than the dielectric constant, the dielectric constant is the dominating the electric field distribution (Metaxas, 1996). Our assumption based on published studies (Birla et al., 2008; Tiwari et al., 2011b; Huang et al., 2015) was that interaction between the loss factor and dielectric constant is negligible, so simulations were run by changing the dielectric constant of the sample from 0.5 to 10 with a fixed loss factor of 0.2 to study the effect of sample dielectric constant on RF heating rate. Similarly, the loss factor of the sample was varied between 0.2 and 20 while the dielectric constant was fixed at 3 to study the effect of sample loss factor on RF heating rate. The sample dielectric properties were selected based on the simulation results shown in table 1.

Effects of Electrode Gap and Top Electrode Voltage on RF Heating Rate

In order to study the effect of electrode gap on RF heating rate, simulations were run by changing the top electrode positions from 90 mm to 130 mm at intervals of 10 mm while the top electrode voltage was considered constant at 8400 V. To study the effect on RF heating rate under a fixed electrode gap of 120 mm, three top electrode voltages (6000, 8400, and 10,000 V) were selected, corresponding to small, medium, and large values.

The relative sensitivity of the simulated heating rate in RF-treated mung beans was evaluated by changing each model parameter by ±20% from the nominal value while the other parameters were held at a fixed value. This method was used with the assumption of no interaction influence of these parameters, which was also assumed in other studies (Birla et al., 2008; Tiwari et al., 2011b; Alfaifi et al., 2014).

Results and Discussion

Simulated Temperature Profiles of Mung Bean

Figure 3 shows the simulated temperature profiles of RF-treated mung beans in three layers along the *z*-axis (*z* = 17, 34, and 50 mm) and in three layers along the *y*-axis (*y* = 0, 110, and 220 mm) at an initial temperature of 20°C after 6 min RF heating with a fixed electrode gap of 120 mm. In the three horizontal layers along the *z*-axis, the average temperature of the bottom, middle, and top layers was 55.1°C, 56.4°C, and 52.7°C, respectively. Since the rectangular container was placed on the center of the bottom elec-

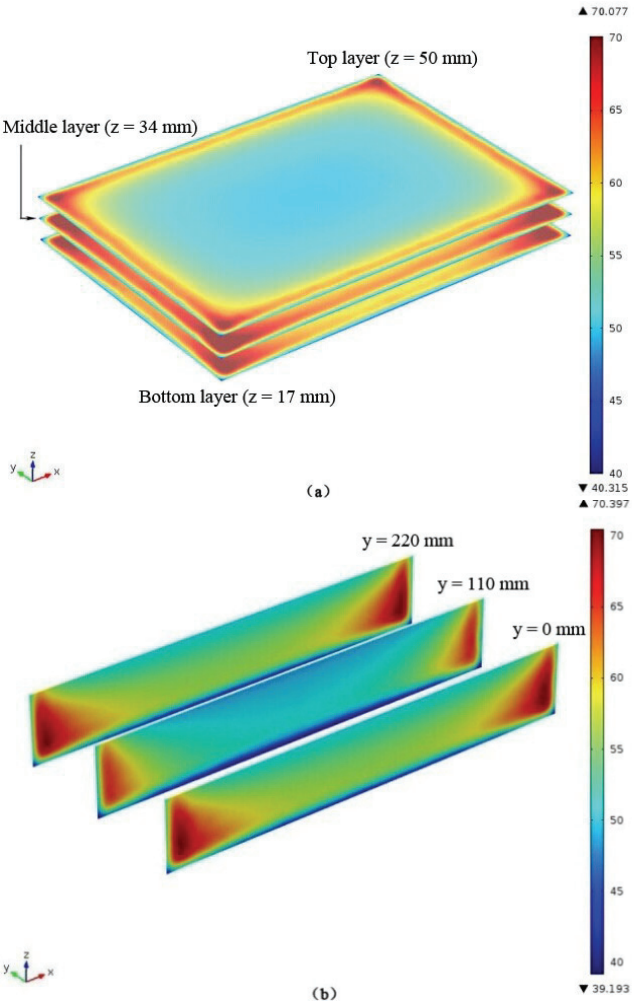

Figure 3. Simulated temperature (°C) profiles of mung beans (300 mm × 220 mm × 50 mm) at (a) three horizontal layers along the *z*-axis (*z* = 17, 34, and 50 mm) and (b) three vertical layers along the *y*-axis (*y* = 0, 110, and 220 mm) after 6 min RF heating with an electrode gap of 120 mm at initial temperature of 20°C.

trode, the sample temperatures in the middle and bottom layers were higher than those in the top layer. The relatively lower temperature in the bottom layer was probably caused by heat loss from the sample to the bottom electrode plate through the container. The low temperatures observed at the outer surfaces of the sample might be attributable to convective heat loss between the outer surfaces of the mung beans and the surrounding air (20°C). In the three vertical layers along the *y*-axis, the temperature increased symmetrically from the center layer (y = 110 mm) to the outer layers of the mung beans sample. The mean sample temperatures in the center layer (y = 110 mm) was 52.7°C, while the mean temperature in the outer layers (y = 0 and 220 mm) was 62.9°C. Generally, the highest temperatures were located at the four corners and edges. This temperature non-uniformity in the mung bean sample could be attributed to the horn effect and the reflection of the electric field at interfaces, which might result in the electric field concentrating at the corners, edges, and lower sections of the sample (Tiwari et al., 2011b). On the other hand, the loss factor of mung beans increased progressively with the increase in temperature (table 1), and hot spots became hotter due to more absorbed RF energy, as indicated by equation 6. Similar heating patterns have been observed for polyurethane foam sheets (Wang et al., 2007a, 2007b), wheat flour (Tiwari et al., 2011b), and raisins (Alfaifi et al., 2014) when subjected to RF treatment.

Comparisons between Experimental and Simulated Temperature Profiles

Figure 4 shows a comparison between the experimental and simulated surface temperature distributions of mung beans in all three layers, and figure 5 shows temperature profiles along the center line (A-A) of each layer. Both results demonstrate that the simulated temperature distribution patterns for all layers were in good agreement with the experimental patterns. Overheating of the corners and edges was observed in both the simulated and experimental temperature distributions. The average temperature differences along the A-A line were 0.35°C, 0.37°C, and 0.01°C for the top, middle, and bottom layers, respectively (fig. 5). The simulated temperatures were slightly higher than the experimental values, probably due to slight heat loss from the experimental samples to the environment before temperature mapping. Good agreement between simulated and experimental temperatures was found again at the center of the middle layer (geometric center) with a high coefficient of determination (R^2 = 0.9997) (fig. 6). The validated simulation model was further used to determine the effects of model parameters on the heating rate of mung beans during RF treatment.

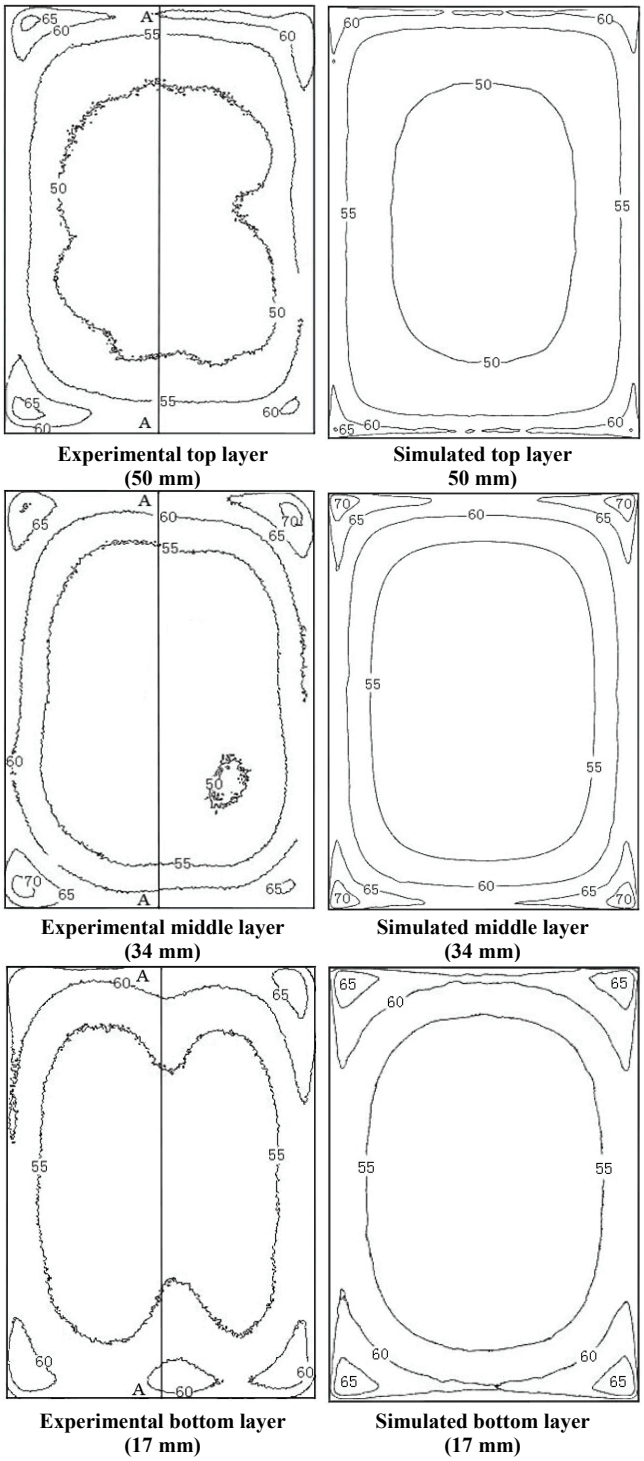

Figure 4. Experimental and simulated temperature distributions (°C) of mung beans in the top, middle, and bottom layers (50, 34, and 17 mm from bottom of sample) placed in a polypropylene container (300 mm × 220 mm × 50 mm) on the center of the bottom electrode after 6 min RF heating with an initial temperature of 20°C and a fixed electrode gap of 120 mm.

Influence of Moisture Content, Density, Specific Heat Capacity, and Thermal Conductivity on RF Heating Rate

Figure 7a shows the influence of sample moisture content on the heating rate of mung beans at the center of the middle layer (34 mm from bottom of sample) when subjected to 6 min RF heating with an electrode gap of 120 mm. The simulation results show that the heating rate increased dramatically with increasing sample moisture content (<18% w.b.) but then slightly decreased with moisture content (>18% w.b.). This behavior could be caused by the increased thermal and dielectric properties of samples with increasing moisture content: the higher the sample moisture content, the larger the thermal conductivity, spe-

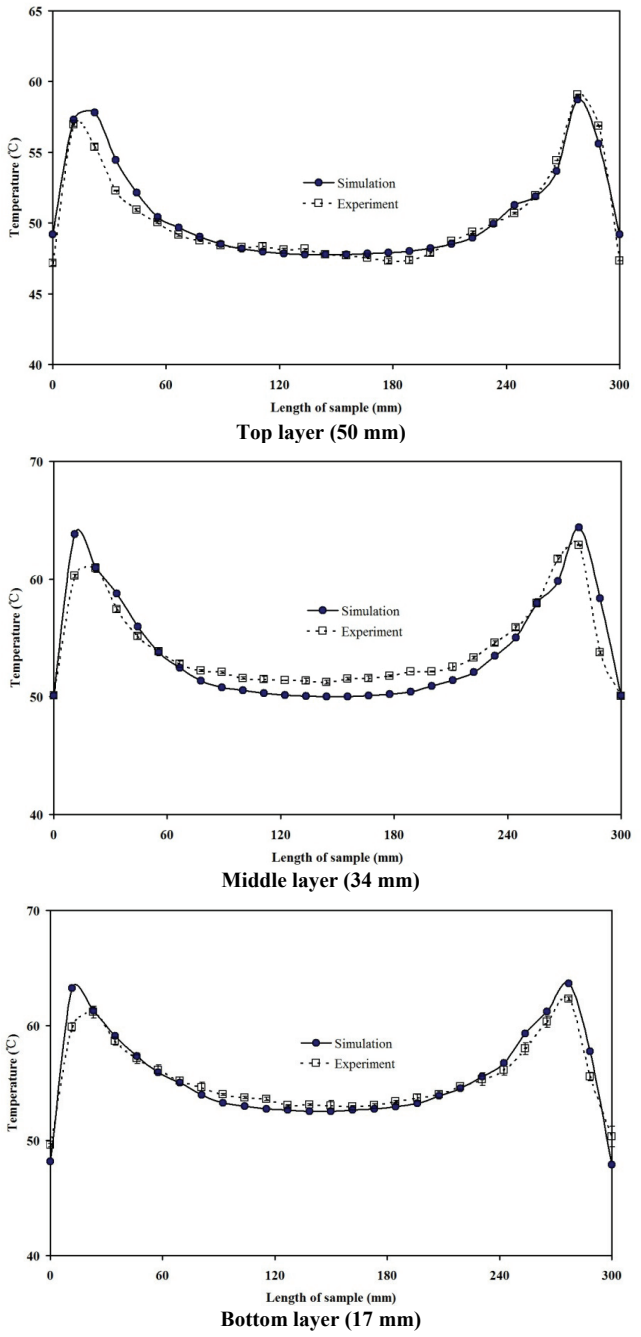

Figure 5. Comparison between experimental and simulated temperature profiles of mung beans along the center line (A-A in fig. 4) in the top, middle, and bottom layers (50, 34, and 17 mm from bottom of sample) placed in a polypropylene container (300 mm × 220 mm × 50 mm) on the center of the bottom electrode after 6 min RF heating with an initial temperature of 20°C and a fixed electrode gap of 120 mm.

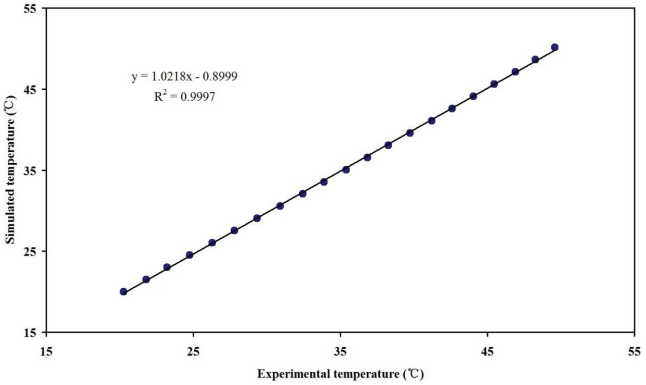

Figure 6. Comparisons of experimental and simulated temperatures (°C) of mung beans at the center of the middle layer (34 mm from bottom of sample) during 6 min RF heating with an electrode gap of 120 mm.

cific heat capacity, dielectric constant, and loss factor of the sample (Guo et al., 2010; Jiao et al., 2011a). Because the RF heating rate was also inversely proportional to the sample dielectric properties, density, and specific heat capacity, the heating rate reached a peak value at around 18% moisture content under the given conditions. It is possible to obtain the appropriate RF heating rate in samples by controlling the sample moisture content under a given electric field intensity (Jiao et al., 2011b). Although the moisture content of dried agricultural products is relatively low, a small change in moisture content can have a significant impact on RF heating rate. The RF heating rate changed by 40% when the moisture content was changed by 20% (table 2). Similar results have been observed for walnut kernels (Mitcham et al., 2004) and peanut butter (Jiao et al., 2014a) during RF treatment.

For RF drying, this heating behavior could provide an advantage in keeping the sample temperature stable, since the RF power or the heating rate are reduced where moisture is removed. The large heating rate at the corners and edges of the sample could be caused by high moisture content that migrated from the central part due to RF treatment. By adding forced hot air from the bottom electrode to speed up the airflow, moisture at the corners and edges could be reduced, resulting in a lower heating rate and more uniform heating (Wang et al., 2010; Jiao et al., 2012). On the other hand, the dielectric properties of mung beans vary with moisture content, which might have some influence on the effectiveness of RF treatments for insect control. Shrestha and Baik (2013) reported that a lower moisture content of the product may result in greater selective heating of insects. A pretreatment process could be added to reduce the moisture content of the samples to a set level, e.g., 6%, before RF treatment to achieve the required heating uniformity and insect mortality

Figure 7b shows the simulated RF heating rate of mung beans at the center of the middle layer as influenced by different sample densities. The heating rates were about 6.0, 4.8, and 4.0 °C min^{-1} for mung beans densities of 800, 1000, and 1200 kg m^{-3}, respectively. It is clear that lower sample density resulted in higher RF heating rate, as described by equation 5. This could be due to a smaller quantity of sample heated using the same RF power. This suggests that compacting the sample in the corners and loosening the sample in the center might improve the RF heating uniformity in the container. A similar decreasing trend of RF heating rate varying with density was reported by Kannan et al. (2013). The RF heating rate changed by 21% when the sample density was changed by 20% (table 2).

The influence of sample specific heat capacity on RF heating rate was also assessed with the validated simulation

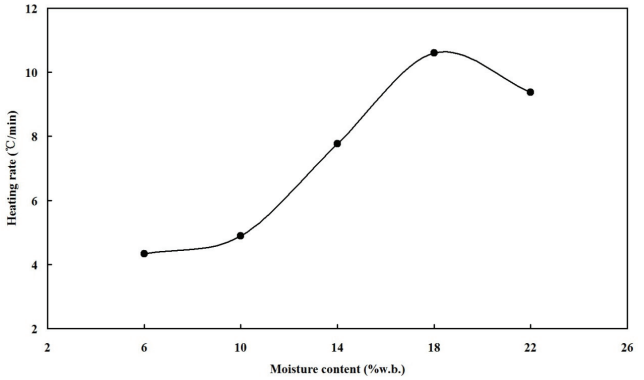

(a)

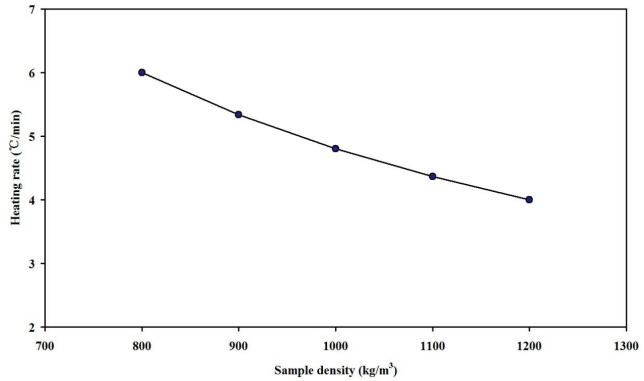

(b)

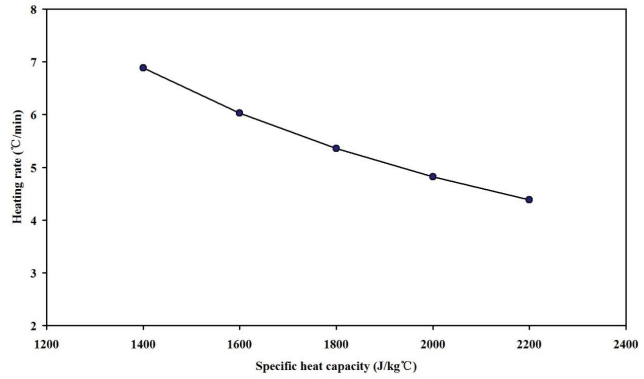

(c)

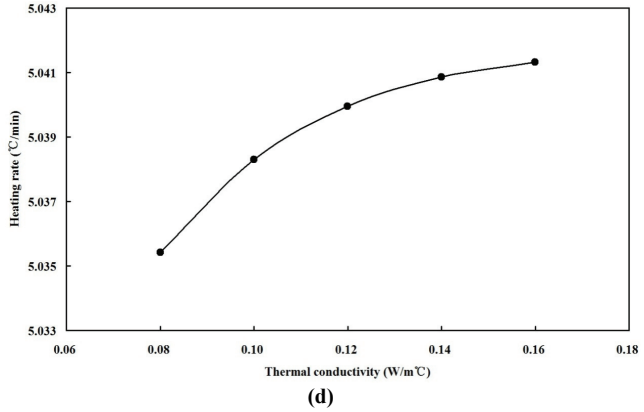

(d)

Figure 7. Simulated heating rate of mung beans at the center of the middle layer (34 mm from bottom of sample) as influenced by (a) sample moisture content, (b) density, (c) specific heat capacity, and (d) thermal conductivity during 6 min RF heating with an electrode gap of 120 mm and a fixed top electrode voltage of 8400 V.

Table 2. Simulated sensitivity of RF heating rate of mung beans with respect to ±20% change in model parameters.

Model Parameter	Nominal Value[a]	Change in Heating Rate
Dielectric properties ($\varepsilon' - j\varepsilon''$)	$(0.021T + 1.82) - j(0.0028T + 0.036)$	74%
Electrode gap (mm)	120	62%
Top electrode voltage (V)	8400	45%
Moisture content (% w.b.)	7.54	40%
Density (kg m^{-3})	953	21%
Specific heat capacity (J kg^{-1} °C^{-1})	$18T + 1165$	19%
Thermal conductivity (W m^{-1} °C^{-1})	0.102	0.35%

[a] T = temperature (°C).

model (fig. 7c). Heating rates were 6.88, 5.35, and 4.38 °C min^{-1} for specific heat capacities of 1400, 1800, and 2200 J kg^{-1} °C^{-1}, respectively. The RF heating rate decreased with increasing sample specific heat capacity, since the sample specific heat capacity is inversely proportional to the RF heating rate in equation 6. This decreasing trend was similar to that for sample density. The RF heating rate changed by 19% when the sample specific heat capacity was changed by 20% (table 2). These results were in good agreement with the observations of Barringer et al. (1994).

Figure 7d shows the general trends of RF heating rate as influenced by sample thermal conductivity during 6 min RF heating with an electrode gap of 120 mm. The RF heating rate increased dramatically and then gradually with the increase in sample thermal conductivity. This could be caused by the fast heat transfer in samples with large thermal conductivity, as shown by equation 2. A similar trend was reported by Bridgwater et al. (1999). However, the influence of sample thermal conductivity on RF heating rate was smaller than the effects of sample moisture content, specific heat capacity, and density, since the RF heating rate changed by only 0.35% when the thermal conductivity of mung beans was changed by 20% (table 2). The effect of thermal conductivity on RF heating rate could be ignored in practical applications.

INFLUENCE OF SAMPLE DIELECTRIC PROPERTIES ON RF HEATING RATE

The simulation results in figure 8a show that the RF heating rate of mung beans was influenced by sample dielectric constant during 6 min RF heating with an electrode gap of 120 mm. The loss factor of the sample was set at 0.2. When the sample dielectric constant increased from 0.5 to 10, the RF heating rate at the center of the middle layer decreased rapidly at first and then slowly. This heating behavior can be illustrated by a monotonic decreasing function with ε' if all other parameters are considered as constant except for ε', as shown in equation 6. The electric field pattern between the two RF electrodes was distorted at the corners and edges of the sample due to the dielectric constant difference between the sample and the air. The electric field distortion could be reduced, resulting in better heating uniformity, by using a surrounding material with a low loss factor and a similar dielectric constant, instead of air (Tiwari et al., 2011b; Jiao et al., 2014b; Huang et al., 2015). Figure 8b shows the trends in RF heating rate of

mung beans as influenced by sample loss factor when the dielectric constant was fixed at 3. The simulation results show that the increase in sample loss factor caused an initial increase and then a reduction in the RF heating rate. Based on equation 6, for a fixed ε′, the maximum heating rate can be obtained as $\pi f \varepsilon_0 V^2/[\rho C_p(\varepsilon' + d_m/d_0)]$ when $\varepsilon'' = \varepsilon' + d_m/d_0$. An increase in ε″ would result in thermal runaway when $\varepsilon'' < \varepsilon' + d_m/d_0$ but would reduce the heating rate when $\varepsilon'' > \varepsilon' + d_m/d_0$.

Figures 8a and 8b both show that the RF heating rate achieved a maximum value when the loss factor was close to the dielectric constant value. In this study, the ε′ and ε″ values were much larger than d_m/d_0, so the maximum heating rate could be achieved when $\varepsilon'' \approx \varepsilon'$. Similar findings have been reported for the influence of sample dielectric properties on RF power distribution in wheat flour (Tiwari et al., 2011b) and peanut butter (Jiao et al., 2014a). The ε′ and ε″ values for all insect (cowpea weevil) stages are higher than those for lentils due to the higher moisture content (70.8%) of insects, which suggests that cowpea weevils would heat at a faster rate than the product (Johnson et al., 2010; Jiao et al., 2011a). The influence of dielectric properties on heating rates has been further applied to predict the differential heating between products and insect pests during RF treatment (Wang et al., 2003; Shrestha and Baik, 2013). Generally, the RF heating rate changed by 74% when the dielectric properties of mung beans by were changed by 20% (table 2). This could be used for predicting the approximate RF heating rate trend by simply considering the dielectric properties of products.

Influence of Top Electrode Voltage and Electrode Gap on RF Heating Rate

Figure 9a shows that a higher top electrode voltage resulted in faster RF heating in mung beans during 6 min RF heating with an electrode gap of 120 mm. When the top electrode voltage varied from 6000 to 10,000 V, the RF heating rate increased from 2.57 to 7.14 °C min^{-1}. This phenomenon could be explained by equations 4 and 5 in which the RF heating rate in products is proportional to the square of the electric field strength (E, V m^{-1}), which is equal to the top electrode voltage since the bottom electrode was grounded. The voltage on the top electrode used in this simulation was estimated by inputting the measured average heating rate using equation 10, and by using computer simulation when the simulated temperature patterns and values matched well with the experimental values (Birla et al., 2008). With the important effect on RF heating rates (table 2), it is essential to precisely determine the top electrode voltage by direct measurement (Zhu et al., 2014).

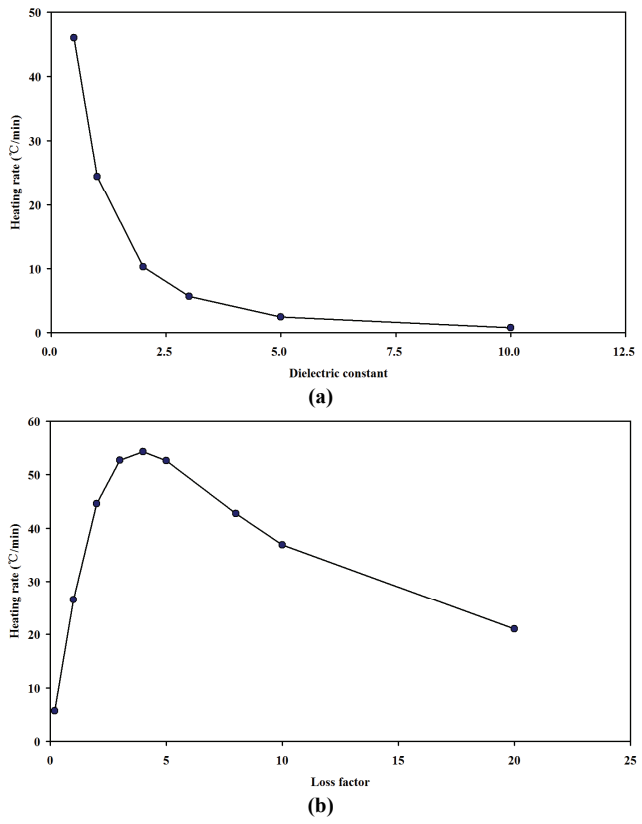

Figure 8. Simulated heating rate of mung beans at the center of the middle layer (34 mm from bottom of sample) with electrode gap of 120 mm, top electrode voltage of 8400 V, sample density of 953 kg m^{-3}, thermal conductivity of 0.102 W m^{-1} °C^{-1}, and specific heat capacity of 18 T + 1165 J kg^{-1} °C^{-1}) as influenced by (a) dielectric constant with loss factor fixed at 0.2 and (b) loss factor with dielectric constant fixed at 3 during 6 min RF heating.

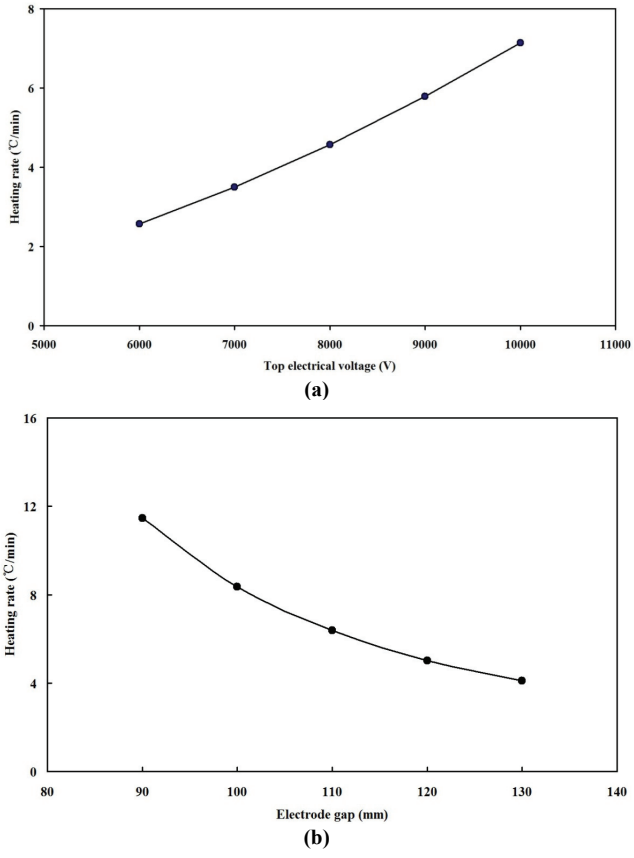

Figure 9. Simulated heating rate of mung beans at the center of the middle layer (34 mm from bottom of sample) with sample moisture content of 7.54% w.b., density of 953 kg m^{-3}, thermal conductivity of 0.102 W m^{-1} °C^{-1}, dielectric properties of (0.021 T + 1.82) – j(0.0028 T + 0.036), and specific heat capacity of 18 T + 1165 J kg^{-1} °C^{-1}) as influenced by (a) top electrode voltage and (b) electrode gap during 6 min RF heating with samples placed on the center of the bottom electrode.

The temperature non-uniformity in the sample could be attributed to the real electric field behavior, which was assumed to be uniformly distributed on the top electrode. In reality, the top electrode voltage could be higher in the corners than in the center, resulting in uneven heating in the sample. This problem could be partially solved by moving the power feed to the center of the top electrode (Wang et al., 2008a).

Figure 9b shows that the RF heating rate was greatly affected by the electrode gap during 6 min RF heating with the top electrode voltage assumed to be 8400 V. The RF heating rate of mung beans decreased as the electrode gap increased from 90 to 130 mm and was inversely proportional to the electrode gap (Jiao et al., 2014a). Since the bottom electrode is normally fixed, the gap between the two electrodes ($d = d_0 + d_m$) can be divided into the air gap (d_0) and the height of the food sample (d_m). For a fixed sample height (d_m), the air gap (d_0) increases and the heating rate decreases with an increasing electrode gap (d), as indicated by equation 6. When the air gap (d_0) is reduced to zero, the value of ε' does not influence the heating rate. As a result, ε'' is the dominating factor in RF heating, and the heating mechanism changes from dielectric heating to resistive heating (Metaxas, 1996). However, an air gap (d_0) is necessary in dielectric heating for use in a continuous system. Rapid heating rates correspond to higher throughputs but may adversely affect the heating uniformity, as indicated by equations 7 to 9. To obtain acceptable heating uniformity and relatively high throughput, an appropriate electrode gap should be selected for RF treatment in industrial applications.

General Applications of Modeling Results

The RF heating rate of mung beans was mostly influenced by sample dielectric properties, followed by the electrode gap, top electrode voltage, sample moisture content, and sample thermal properties (table 2). In a mixture of insects in mung beans, the heating rate of insects would be higher than that of mung beans because the dielectric properties of insects are more than ten times greater than those of mung beans when treated with RF energy (Jiao et al., 2011a). The insects would reach a lethal temperature while the product would be heated to lower temperatures that do not cause quality loss. This is an attractive feature of insect control using RF energy. Differential heating has been reported for both simulations and experiments for insects in walnuts (Wang et al., 2003), almonds (Wang et al., 2013), and wheat (Shrestha and Baik, 2013). By exploring the differences in heating rate between insect pests and host products during RF heating, the required processing time and product temperature could potentially be reduced for effective treatment, resulting in reduced adverse effects on product quality.

The results of the current study indicate that the heating rate increased with increasing voltage, moisture content, and thermal conductivity but with decreasing electrode gap, dielectric constant, density, and heat capacity. The heating uniformity could be improved by reducing the product moisture content, increasing the electrode gap, and compacting the sample in the corners during the RF treatment. Expanding on the simulation results, a surrounding material with a dielectric constant similar to that of the sample could further reduce overheating of the corners. If the heating uniformity is still not enough for controlling insects without damaging the product quality, taking the simulation results from this study into consideration, then additional hot air surface heating, sample movement, and/or mixing could be used to ensure RF heating uniformity in industrial applications.

Conclusion

A computer model of RF heating of mung beans was developed for a 6 kW, 27.12 MHz free-running oscillator RF system using COMSOL software and then validated with experimental results. The simulation and experimental results both showed higher temperatures in the middle layers of samples, and corners were heated more than center areas in all layers. The simulation results confirmed that the specific heat capacity and density of the sample affected the RF heating rate with similar trends, and a loss factor equal to the dielectric constant provided fast RF heating. A proper selection of sample moisture content, electrode gap, and top electrode voltage might be useful to reduce the concentration of the electric field at the corners and edges of the sample. The developed model is an effective tool to guide a reasonable selection of RF treatment conditions based on different RF heating rates, thereby improving the heating uniformity of dried products exposed to RF treatment and understanding the complex RF heating process.

Acknowledgements

This research was conducted in the College of Mechanical and Electronic Engineering, Northwest A&F University, and supported by research grants from the 948 Program of the Ministry of Agriculture of China (2014-Z21), the PhD Programs Foundation of the Ministry of Education of China (Grant No. 20120204110022) and the General Program of the National Natural Science Foundation of China (Grant No. 31371853). The authors thank Qian Hao, Rongjun Yan, Bo Ling, Rui Li, and Lixia Hou for their help in conducting the experiments.

References

Alfaifi, B., Tang, J., Jiao, Y., Wang, S., Rasco, B., Jiao, S., & Sablani, S. (2014). Radio frequency disinfestation treatments for dried fruit: Model development and validation. *J. Food Eng., 120*, 268-276. http://dx.doi.org/10.1016/j.jfoodeng.2013.07.015.

Amarteifio, J. O., & Moholo, D. (1998). The chemical composition of four legumes consumed in Botswana. *J. Food Comp. Analysis, 11*(4), 329-332. http://dx.doi.org/10.1006/jfca.1998.0595.

Barber, H. (1983). Chapter 8: Dielectric heating. In H. Barber (Ed.), *Electroheat.* New York, N.Y.: Granada Publishing.

Barreveld, W. H. (1993). Date palm products. FAO Agricultural Services Bulletin No. 101. Rome, Italy, United Nations FAO.

Barringer, S., Davis, E., Gordon, J., Ayappa, K., & Davis, H. (1994). Effect of sample size on the microwave heating rate: Oil vs. water. *AIChE J., 40*(9), 1433-1439. http://dx.doi.org/10.1002/aic.690400902.

Berbert, P. A., Queriroz, D. M., & Melo, E. C. (2002). Dielectric properties of common bean. *Biosyst. Eng., 83*(4), 449-462. http://dx.doi.org/10.1006/bioe.2002.0135.

Birla, S. L., Wang, S., Tang, J., & Hallman, G. (2004). Improving heating uniformity of fresh fruit in radio frequency treatments for pest control. *Postharvest Biol. Tech., 33*(2), 205-217. http://dx.doi.org/10.1016/j.postharvbio.2004.02.010.

Birla, S. L., Wang, S., & Tang, J. (2008). Computer simulation of radio frequency heating of model fruit immersed in water. *J. Food Eng., 84*(2), 270-280. http://dx.doi.org/10.1016/j.jfoodeng.2007.05.020.

Bridgwater, A., Meier, D., & Radlein, D. (1999). An overview of fast pyrolysis of biomass. *Organic Geochem., 30*(12), 1479-1493. http://dx.doi.org/10.1016/S0146-6380(99)00120-5.

Carpenter, J., Gianessi, L., & Lynch, L. (2000). The economic impact of the scheduled U.S. phaseout of methyl bromide. Washington, D.C.: National Center for Food and Agricultural Policy.

Chan, T., Tang, J., & Younce, F. (2004). 3-Dimensional numerical modeling of an industrial radio frequency heating system using finite elements. *J. Microwave Power Electromag. Energy, 39*(2), 87-105.

Choi, C., & Konrad, A. (1991). Finite-element modeling of the RF heating process. *IEEE Trans. Magnetics, 27*(5), 4227-4230. http://dx.doi.org/10.1109/20.105034.

COMSOL. (2012). COMSOL Multiphysics. V4.3a. Burlington, Mass.: COMSOL, Inc.

Guo, W., Wang, S., Tiwari, G., Johnson, J. A., & Tang, J. (2010). Temperature and moisture dependent dielectric properties of legume flour associated with dielectric heating. *LWT - Food Sci. Tech., 43*(2), 193-201. http://dx.doi.org/10.1016/j.lwt.2009.07.008.

Hallman, G., & Sharp, J. (1994). Radio frequency heat treatments. In J. L. Sharp, & G. I. Hallman (Eds.), *Quarantine Treatments for Pests of Food Plants.* Boulder, Colo.: Westview Press.

Huang, Z., Zhu, H., Yan, R., & Wang, S. (2015). Simulation and prediction of radio frequency heating in dry soybeans. *Biosyst. Eng., 129*, 34-47. http://dx.doi.org/10.1016/j.biosystemseng.2014.09.014.

Hui, L., & Ninghui, L. (2013). Situation of China's mung bean trade and its trend prospect. *Agric. Outlook, 2013*(issue 6), 62-64.

Ikediala, J., Hansen, J., Tang, J., Drake, S., & Wang, S. (2002). Development of a saline water immersion technique with RF energy as a postharvest treatment against codling moth in cherries. *Postharvest Biol. Tech., 24*(2), 209-221. http://dx.doi.org/10.1016/S0925-5214(02)00018-2.

Jiao, S., Johnson, J., Tang, J., Tiwari, G., & Wang, S. (2011a). Dielectric properties of cowpea weevil, black-eyed peas, and mung beans with respect to the development of radio frequency heat treatments. *Biosyst. Eng., 108*(3), 280-291. http://dx.doi.org/10.1016/j.biosystemseng.2010.12.010.

Jiao, S., Tang, J., Johnson, J., Tiwari, G., & Wang, S. (2011b). Determining radio frequency heating uniformity of mixed beans for disinfestation treatments. *Trans. ASABE, 54*(5), 1847-1855. http://dx.doi.org/10.13031/2013.39824.

Jiao, S., Johnson, J. A., Tang, J., & Wang, S. (2012). Industrial-scale radio frequency treatments for insect control in lentils. *J. Stored Prod. Res., 48*, 143-148. http://dx.doi.org/10.1016/j.jspr.2011.12.001.

Jiao, Y., Tang, J., Wang, S., & Koral, T. (2014a). Influence of dielectric properties on the heating rate in free-running oscillator radio frequency systems. *J. Food Eng., 120*, 197-203. http://dx.doi.org/10.1016/j.jfoodeng.2013.07.032.

Jiao, Y., Tang, J., & Wang, S. (2014b). A new strategy to improve heating uniformity of low-moisture foods in radio frequency treatment for pathogen control. *J. Food Eng., 141*, 128-138. http://dx.doi.org/10.1016/j.jfoodeng.2014.05.022.

Johnson, J., Valero, K., Wang, S., & Tang, J. (2004).Thermal death kinetics of red flour beetle (Coleoptera: Tenebrionidae). *J. Econ. Entomol., 97*(6), 1868-1873. http://dx.doi.org/10.1603/0022-0493-97.6.1868.

Johnson, J., Wang, S., & Tang, J. (2010). Radio frequency treatments for insect disinfestation of dried legumes. In *Proc. 10th Intl. Working Conf. Stored Product Protection* (pp. 688-694). Berlin, Germany: Julius Kühn Institut. Retrieved from http://pub.jki.bund.de/index.php/JKA/article/view/575.

Kannan, S., Dev, S. R., Gariepy, Y., & Raghavan, G. (2013). Effect of radio frequency heating on the dielectric and physical properties of eggs. *Prog. Electromag. Res. B, 51*, 201-220. http://dx.doi.org/10.2528/PIERB13031812.

Lagunas-Solar, M., Pan, Z., Zeng, N., Truong, T., Khir, R., & Amaratunga, K. (2007). Application of radio frequency power for non-chemical disinfestation of rough rice with full retention of quality attributes. *Appl. Eng. Agric., 23*(5), 647-654. http://dx.doi.org/10.13031/2013.23661.

Marra, F., Lyng, J., Romano, V., & McKenna, B. (2007). Radio frequency heating of foodstuff: Solution and validation of a mathematical model. *J. Food Eng., 79*(3), 998-1006. http://dx.doi.org/10.1016/j.jfoodeng.2006.03.031.

Metaxas, A. (1996). *Foundations of Electroheat: A Unified Approach.* New York, N.Y.: John Wiley.

Mitcham, E., Veltman, R., Feng, X., De Castro, E., Johnson, J., Simpson, T., Biasi, W., Wang, S., & Tang, J. (2004). Application of radio frequency treatments to control insects in in-shell walnuts. *Postharvest Biol. Tech., 33*(1), 93-100. http://dx.doi.org/10.1016/j.postharvbio.2004.01.004.

Nelson, S. (1996). Review and assessment of radio frequency and microwave energy for stored-grain insect control. *Trans. ASAE, 39*(4), 1475-1484. http://dx.doi.org/10.13031/2013.27641.

Neophytou, R. I., & Metaxas, A. C. (1996). Computer simulation of a radio frequency industrial system. *J. Microwave Power Electromag. Energy, 31*(4), 251-259.

Neophytou, R. I., & Metaxas, A. C. (1998). Combined 3D FE and circuit modeling of radio frequency heating systems. *J. Microwave Power Electromag. Energy, 33*(4), 243-262.

Osteen, C. D. (2000). Economic implications of the methyl bromide phaseout. Economic Research Service No. 756. Washington, D.C.: USDA.

Pimentel, D. (2002). Postharvest pest losses. In *Encyclopedia of Pest Management* (pp. 654-656). Boca Raton, Fla.: CRC Press.

Piyasena, P., Dussault, C., Koutchma, T., Ramaswamy, H., & Awuah, G. (2003). Radio frequency heating of foods: Principles, applications, and related properties: A review. *Crit. Rev. Food Sci. Nutr., 43*(6), 587-606. http://dx.doi.org/10.1080/10408690390251129.

Ravikanth, L., Jayas, D., Alagusundaram, K., & Chelladurai, V. (2012). Measurement of thermal properties of mung bean (*Vigna radiata*). *Trans. ASABE, 55*(6), 2245-2250. http://dx.doi.org/10.13031/2013.42481.

Romano, V., & Marra, F. (2008). A numerical analysis of radio frequency heating of regular-shaped foodstuff. *J. Food Eng., 84*(3), 449-457. http://dx.doi.org/10.1016/j.jfoodeng.2007.06.006.

Shrestha, B., & Baik, O.-D. (2013). Radio frequency selective heating of stored-grain insects at 27.12 MHz: A feasibility study. *Biosyst. Eng., 114*(3), 195-204. http://dx.doi.org/10.1016/j.biosystemseng.2012.12.003.

Tiwari, G., Wang, S., Tang, J., & Birla, S. (2011a.). Computer simulation model development and validation for radio frequency (RF) heating of dry food materials. *J. Food Eng., 105*(1), 48-55. http://dx.doi.org/10.1016/j.jfoodeng.2011.01.016.

Tiwari, G., Wang, S., Tang, J., & Birla, S. (2011b). Analysis of radio frequency (RF) power distribution in dry food materials. *J. Food Eng., 104*(4), 548-556. http://dx.doi.org/10.1016/j.jfoodeng.2011.01.015.

Wang, S., Tang, J., Cavalieri, R., & Davis, D. (2003). Differential heating of insects in dried nuts and fruits associated with radio frequency and microwave treatments. *Trans. ASAE, 46*(4), 1175-1184. http://dx.doi.org/10.13031/2013.13941.

Wang, S., Monzon, M., Johnson, J., Mitcham, E., & Tang, J. (2007a). Industrial-scale radio frequency treatments for insect control in walnuts: I: Heating uniformity and energy efficiency. *Postharvest Biol. Tech., 45*(2), 240-246. http://dx.doi.org/10.1016/j.postharvbio.2006.12.023.

Wang, S., Monzon, M., Johnson, J., Mitcham, E., & Tang, J. (2007b). Industrial-scale radio frequency treatments for insect control in walnuts: II: Insect mortality and product quality. *Postharvest Biol. Tech., 45*(2), 247-253. http://dx.doi.org/10.1016/j.postharvbio.2006.12.020.

Wang, S., Luechapattanaporn, K., & Tang, J. (2008a). Experimental methods for evaluating heating uniformity in radio frequency systems. *Biosyst. Eng., 100*(1), 58-65. http://dx.doi.org/10.1016/j.biosystemseng.2008.01.011.

Wang, S., Yue, J., Chen, B., & Tang, J. (2008b). Treatment design of radio frequency heating based on insect control and product quality. *Postharvest Biol. Tech., 49*(3), 417-423. http://dx.doi.org/10.1016/j.postharvbio.2008.02.004.

Wang, S., Tiwari, G., Jiao, S., Johnson, J., & Tang, J. (2010). Developing postharvest disinfestation treatments for legumes using radio frequency energy. *Biosyst. Eng., 105*(3), 341-349. http://dx.doi.org/10.1016/j.biosystemseng.2009.12.003.

Wang, S., Tang, J., Johnson, J., & Cavalieri, R. (2013). Heating uniformity and differential heating of insects in almonds associated with radio frequency energy. *J. Stored Prod. Res., 55*, 15-20. http://dx.doi.org/10.1016/j.jspr.2013.06.003.

Yang, J., Zhao, Y., & Wells, J. H. (2003). Computer simulation of capacitive radio frequency (RF) dielectric heating on vegetable sprout seeds. *J. Food Proc. Eng., 26*(3), 239-263. http://dx.doi.org/10.1111/j.1745-4530.2003.tb00600.x.

Zhu, H., Huang, Z., & Wang, S. (2014). Experimental and simulated top electrode voltage in free-running oscillator radio frequency systems. *J. Electromag. Waves Appl., 28*(5), 606-617. http://dx.doi.org/10.1080/09205071.2014.881724.